Progress In Electromagnetics Research B, Vol. 23, 131–146, 2010

MODELING AND CHARACTERIZATION OF FREQUENCY AND TEMPERATURE VARIATION OF COMPLEX PERMEABILITY OF FERRITE LTCC MATERIAL

N. Blaž, A. Marić, G. Radosavljević, L. Živanov and G. Stojanović

Faculty of Technical Sciences
University of Novi Sad
Trg Dositeja Obradovića 6, 21000 Novi Sad, Serbia

I. Atassi and W. Smetana

Institute of Sensor and Actuator Systems
Vienna University of Technology
Gusshausstrasse 27-29/366-AEM, A-1040 Vienna, Austria

Abstract—This paper presents modeling of the complex permeability spectra, fabrication and a wide frequency range characterization of a toroidal LTCC ferrite sample. A commercial ferrite tape ESL 40012 is used, and standard LTCC (Low Temperature Co-fired Ceramic) processing has been applied to the sample fabrication. The characterization was performed using a short coaxial sample holder and a vector network analyzer in the frequency range from 300 kHz to 1 GHz, at different temperatures. Using the model of the complex permeability spectra dispersion parameters of ferrite LTCC material has been determined for various temperatures. Characteristics of test samples are compared with modeled results and commercially available toroid made of similar NiZn ferrite material.

1. INTRODUCTION

A magnetic permeability characterization is very important for ferrite component design. Knowledge of this parameter can be applied to circuit design and wave transmission calculations. The important radio and microwave magnetic materials are mainly thin films and

Received 11 June 2010, Accepted 8 July 2010, Scheduled 16 July 2010
Corresponding author: N. Blaž (nelu@uns.ac.rs).

nonconductor forms such as powdered-iron suspensions and ferrites. These materials have many important properties and require different measurements for their characterization.

The measurement of ferrite permeability is necessary for engineers to design and choose ferrite properly. The inductance of ferrite core inductors depends not only on the number or geometry of winding wires, but also on the permeability of the ferrite core. However, at high frequencies direct measurement of the permeability is difficult. The commonly used methods for magnetic material determination are the transmission/reflection method [1–7], equivalent circuit model method [8, 9] and resonant method [10].

In [8], the frequency dependent RLC equivalent circuit parameters (impedance, resonant frequency, resonant impedance and quality factor), as well as the effective permeability of the ferrite core, are extracted from measurement. It is assumed that the capacitance of the equivalent circuit is invariant with frequency. The impedance measurement is accomplished using an impedance analyzer. Another extraction method presented in [9] requires the assumption that the inductance of the equivalent circuit does not change significantly with frequency when the frequency is lower than the roll off frequency of core permeability. The equivalent circuit parameters of the inductor were then derived by measuring the resonant frequencies of two different inductor circuits which resonant frequencies are close to each other. Due to the assumptions mentioned above, the upper frequency limitation of this method is the inductor's self-resonant frequency. The measurements must be accomplished using both a network analyzer and RF LCR meter.

When we need to determine the relative permeability in high frequency range extending to 1 GHz or even higher we used a vector network analyzer (VNA) and a coaxial sample holder [11, 12]. A simple experimental method to determine the initial complex permeability of the toroidal type ferrite core using thoroughly designed fixtures is introduced. With the ferrite core installed in a shorted coaxial line, the fixture forms a one turn inductor or a shorted transmission line with distributed parameters. The relative permeability of the ferrite can then be extracted from S_{11} of the coaxial test holder with the aid of the vector network analyzer. Also, described detailed compensation process is similar to the method presented in [13]. A coaxial measurement cell usually consists of specially shaped composite geometry partially filled with material sample [14–16]. Coaxial discontinuity structures are widely used as an element of microwave devices and commonly used in the permeability and/or permittivity measurement for materials [17].

The intrinsic complex permeability is the critical parameter for optimized design, especially in the high-frequency applications. In order to achieve better performance of ferrite components, the possibility of their production in LTCC technology [18–21] is quite attractive from a system design and manufacturing point of view. For the design of LTCC ferrite components such as EMI filters inductors and transformers, it is important to be familiar with real and imaginary parts of the complex permeability of LTCC tape [22–24]. The magnetometer setup in [22] consists of a coplanar transmission line on a low-loss printed circuit board with two coils to ground. The ferrite sample is used as core in the coils. From an S-parameter transmission measurement of the circuit without and with the ferrite sample the quotient of the empty and filled coil impedances can be calculated. Magnetic permeability of NiZn-ferrite measured on unconstrained sintered rings, constrained sintered ferrite in a LTCC stack with Dupont 951 and susceptibility measured on cubes for the sintering temperatures of 940°C. In [23], LTCC ferrite combined with screen printable silver conductor and low permeability dielectric produce small, low power, low profile transformers — with no wire or discrete core. The resulting transformers can be used for power applications under 1 W that require galvanic isolation. Typical applications include isolated power for sensors, RS-232 or 485 circuits, data acquisition and even digitally-interfaced modems. In [24], only frequency variation of the complex permeability modulus of ferrite tape ESL 40010 is demonstrated, but variation of the real and imaginary parts of the complex permeability is not presented.

Frequency variation of the real and imaginary parts of the complex permeability of ferrite LTCC materials obtained by the short coaxial line method is presented in this paper. A theoretical dispersion model of complex permeability is given in Section 2. The experimental technique for measuring the complex permeability of the toroidal sample, based on the short coaxial line method in the frequency range from 300 kHz to 1 GHz is presented in Section 3. The designed sample was fabricated in the standard LTCC technology. A simple holder method for high frequency measurement of S-parameters of toroidal magnetic samples is shown in Section 4. In Section 5, the determination of the complex permeability spectra for ferrite LTCC tape ESL 40012 [25] is presented. For better overview of test sample characteristics, in Section 6, LTCC toroid parameters are compared to parameters of commercial available ferrite core. A short summary of obtained results and conclusion is presented in Section 7.

2. THEORETICAL DISPERSION MODEL

Complex permeability of ferrites is important factor and many investigations have been carried out in experimental and theoretical bases, [26–28]. In the frequency range from RF to microwave, the permeability spectra of ferrite materials can be characterized by different magnetizing mechanisms domain-wall motion, magnetization rotation, and gyromagnetic spin rotation.

It is well-known that permeability spectra of polycrystalline ferrites can be decomposed into a spin rotational component χ_{spin} and domain wall component $\chi_{dw.}$

$$\mu = 1 + \chi_{spin} + \chi_{dw}. \tag{1}$$

The spin rotational component is of relaxation type (due to large damping factor of spin rotation in the ferrite), and its dispersion is inversely proportional to the frequency. The domain wall component is of resonance type and depends on the square of frequency. Each component can be shown, as in [27], in the following form

$$\chi_{spin} = \frac{K_{spin}}{1 + i\frac{\omega}{\omega_{spin}^{res}}}, \tag{2}$$

$$\chi_{dw} = \frac{K_{dw}\left(\omega_{dw}^{res}\right)^2}{\left(\omega_{dw}^{res}\right)^2 - \omega^2 + i\beta\omega}, \tag{3}$$

where ω is the operating frequency; K_{spin} is the static spin susceptibility; ω_{spin}^{res} is the spin resonance frequency; K_{dw} is the static susceptibility of domain wall motion; ω_{dw}^{res} is the domain wall resonance frequency; β is the damping factor of the domain wall motion. If Equations (2) and (3) have been included in (1), and real and imaginary parts of permeability have been separated, they can be expressed as

$$\mu' = 1 + \frac{K_{spin}\left(\omega_{spin}^{res}\right)^2}{\left(\omega_{spin}^{res}\right)^2 + \omega^2} + \frac{K_{dw}\left(\omega_{dw}^{res}\right)^2\left(\left(\omega_{dw}^{res}\right)^2 - \omega^2\right)}{\left(\left(\omega_{dw}^{res}\right)^2 - \omega^2\right)^2 + \beta^2\omega^2}, \tag{4}$$

$$\mu'' = \frac{K_{spin}\omega_{spin}^{res}\omega}{\left(\omega_{spin}^{res}\right)^2 + \omega^2} + \frac{K_{dw}\left(\omega_{dw}^{res}\right)^2\beta\omega}{\left(\left(\omega_{dw}^{res}\right)^2 - \omega^2\right)^2 + \beta^2\omega^2}. \tag{5}$$

That means that complete permeability spectra can be described by the superposition of spin rotation and domain wall motion components. In this paper, dispersion parameters $K_{spin}, \omega_{spin}^{res}, K_{dw}, \omega_{dw}^{res}$ and β can be determined by numerical fitting of the measurement obtained μ' and μ'' spectra to Equations (4) and (5).

3. MEASUREMENT TECHNIQUE

In this paper, in order to determine the complex permeability of toroidal-shape samples, measurements of S-parameters have been performed using the E5071B *Agilent Technology* vector network analyzer. A coaxial line method is the most commonly used method [11, 12] for high frequency measurement of complex permeability. For this purpose a coaxial line cell has been used. The sample holder consists of a conductive shield surrounding the central conductor, which terminates in short circuit, as can be seen in Figure 1. The holder has $50\,\Omega$ characteristic impedance and is terminated with a standard APC-7 connector. The short circuit produces a maximum magnetic field and a minimum electric field near the sample, thus making the short circuit technique particularly suite for the measurement of permeability of the test sample. The medium between the inner and outer conductors of the cell is air. The height b of the outer conductor is 24,5 mm, which obeys the condition $b < \lambda/4$ for maximal frequency ($f = 1\,\text{GHz}$) in order to avoid the $\lambda/4$ resonant effect.

The coaxial sample holder (with and without sample) is connected to the calibrated network analyzer through the $50\,\Omega$ coaxial cable. The analyzer supplies an electromagnetic wave propagating in a Transverse Electro-Magnetic (TEM) mode. The reflection coefficient is measured, permitting the determination of the input impedance of the cell with

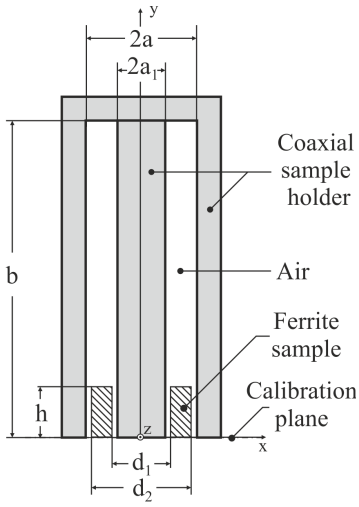

Figure 1. Cross section of the sample holder with toroidal sample.

sample. Equation for determination of the complex permeability of the holder equipped with the test sample is derived in [29]. Since the construction of this holder creates one turn around the toroid (see Figure 1), the complex magnetic flux of the measured circuit including the ring core is given by the equation

$$\tilde{\Phi} = \iint\limits_{S} \vec{B} \cdot d\vec{S} = \int\limits_{0}^{a} \int\limits_{0}^{b} \frac{\mu_0 \mu_r I}{2\pi x} dx dy. \tag{6}$$

By dividing the surfaces of cross section into the holder complex flux density is given by Equation (6), where $\vec{B}$ presents the complex phasor-vector of magnetic flux density; μ_0 stands for the permeability of free space; μ_r is the relative permeability of sample; I is the complex phasor of harmonic time-dependent electrical current $i(t)$.

The magnetic flux of measured circuit is then

$$\tilde{\Phi} = \frac{\mu_0 I}{2\pi} \left\{ (\tilde{\mu}_r - 1) h \cdot \ln\left(\frac{d_2}{d_1}\right) + b \cdot \ln\left(\frac{a}{a_1}\right) \right\}, \tag{7}$$

and the complex susceptibility of the sample under test is given by equation

$$\tilde{\chi} = \frac{2\pi \left(\tilde{\Phi} - \tilde{\Phi}_{air}\right)}{hI\mu_0 \cdot \ln\left(\frac{d_2}{d_1}\right)}, \tag{8}$$

where $\tilde{\Phi}_{air}$ is a magnetic flux when ferrite core is not mounted in the holder

$$\tilde{\Phi}_{air} = \frac{b\mu_0 I}{2\pi} \ln\left(\frac{a}{a_1}\right). \tag{9}$$

The measured complex impedance Z of an equivalent electric circuit of the cell loaded with the ferrite core shown in Figure 1 can be defined as $\tilde{Z} = R + j\omega L = j\omega\tilde{\Phi}/I$. Instead of fluxes $\tilde{\Phi}$ and $\tilde{\Phi}_{air}$ in Equation (8) corresponding complex impedance $\tilde{Z}$ and $\tilde{Z}_{air}$ measured with and without magnetic core respectively can be used

$$\tilde{\mu}_r = 1 + \tilde{\chi} = 1 + \frac{\left(\tilde{Z} - \tilde{Z}_{air}\right)}{jh \cdot \mu_0 \cdot f \cdot \ln\left(\frac{d_2}{d_1}\right)}, \tag{10}$$

where d_1 and d_2 denote the inner and outer diameters of the toroid, respectively. h is the height of the toroid, and f is the frequency of applied electromagnetic field. The complex permeability is therefore calculated from the difference between the impedance of the cell loaded with the toroidal sample and that without it. The vector network

analyzer measures the complex scatter parameter S_{11}, which is related to the input impedance of the cell (with or without sample) according to the following equation

$$\tilde{Z}_{in} = Z_0 \frac{1 + S_{11}}{1 - S_{11}}. \tag{11}$$

where $Z_0 = 50\,\Omega$ is the characteristic impedance of the 7 mm test port.

The loss tangent can be calculated as the ratio between the imaginary and real parts of complex permeability

$$tg\delta = \frac{\mu_r''}{\mu_r'}. \tag{12}$$

4. FABRICATION AND EXPERIMENTAL CHARACTERIZATION

The sample was fabricated using the standard LTCC technology, following all conventional steps for its realization. The commercial ferrite tape ESL 40012 [25] was used for the sample fabrication, implementing structuring of tapes by means of laser micro-machining, laminating and co-firing the stack of 62 LTCC tape layers. Isostatic lamination of the collated layers was performed at a pressure of 120 bars, for 5 minutes. Firing of the laminated stack has been conducted in a high temperature box furnace at a peak temperature of 885°C and a total firing cycle time of 16 hours. The finalized sample is presented in Figure 2. Dimensions of the ferrite sample are: inner diameter 4 mm, outer diameter 6,6 mm and height 3 mm.

Figure 2. Sample — ESL 40012 LTCC ferrite tape.

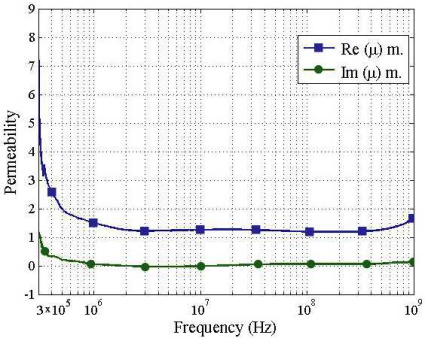

Figure 3. The measured relative complex permeability of a toroidal type Teflon sample using coaxial line method from 300 kHz to 1 GHz.

The S_{11} parameters are obtained through measurement with the vector network analyzer *Agilent* E5071B. The original coaxial line holder HP 04191-85302 was used. In comparison with some other coaxial techniques that are widely used [1–6], elimination of undesirable influences, such as optimization and phase compensation, is not needed. Permeability of the test sample can be obtained by measuring the input impedance differences between the short coaxial sample holder loaded with a toroidal sample and that without it.

To validate the test accuracy and effectiveness of the proposed technique, a toroidal type Teflon sample (dimension: inner diameter 4 mm, outer diameter 6,6 mm and height 3 mm) was measured using coaxial line method, as shown in Figure 3. It can be seen that the coaxial line method achieve satisfactory accuracy below 1 GHz.

Real and imaginary parts of scattering parameter S_{11} are measured with LTCC ferrite sample (Re(S_{11}), Im(S_{11})) and without sample (Re0(S_{11}), Im0(S_{11})), Figure 4, in frequency range from 300 kHz to 1 GHz.

Complex permeability is calculated from measured S-parameters using Equations (10) and (11). Real and imaginary parts of ESL 40012 permeability are depicted in Figure 5.

The maximum value (700) of the real part of permeability is at 2,1 MHz. The imaginary part of permeability reaches its maximum value (330) at 7 MHz. Intersection of these two characteristics is at 9,3 MHz.

Permeability modulus is presented in Figure 6 and its peak is 708 at 2,5 MHz. Using Equation (12) the loss tangent is calculated and presented in Figure 7.

To support measured results a reference measurement was

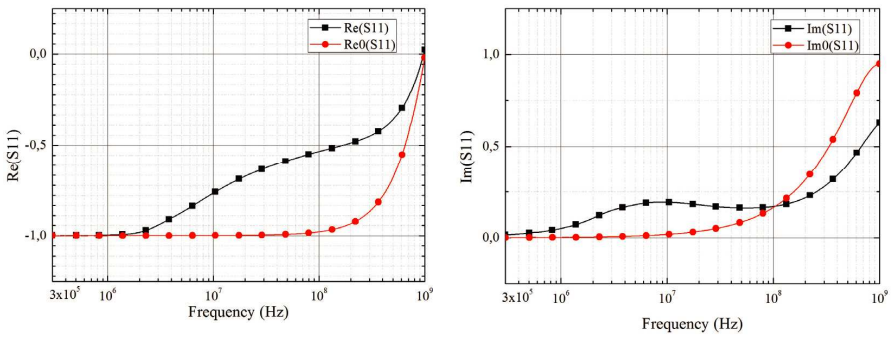

Figure 4. Measured Re(S_{11}) (a) and Im(S_{11}) (b) with and without sample in the coaxial holder.

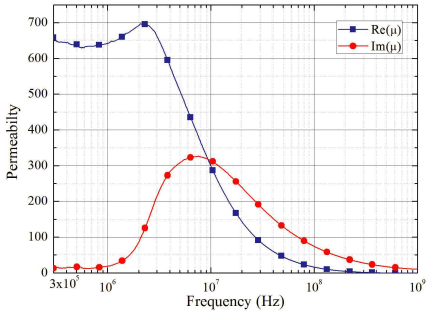

Figure 5. Real and imaginary parts of permeability for ESL 40012.

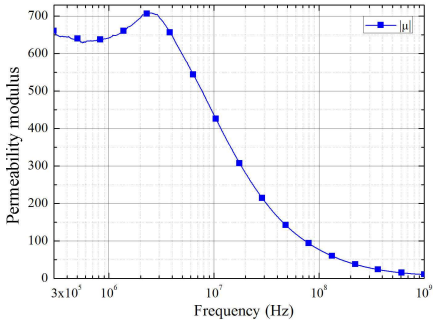

Figure 6. Permeability modulus of the ferrite tape ESL 40012.

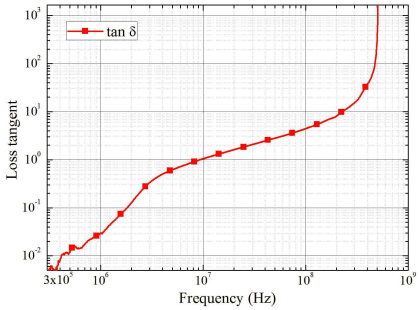

Figure 7. Loss tangent of the ferrite tape ESL 40012.

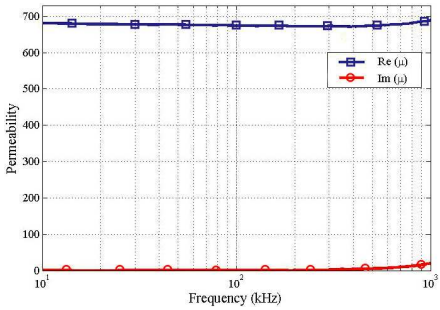

Figure 8. Real and imaginary parts of permeability for ESL 40012 at low frequency (10 kHz–1000 kHz).

performed at low frequency (10 kHz–1000 kHz) using a simpler LCZ meter (HP 4277) and discrete turns of wire, [12], Figure 8. This approach has some major disadvantages. First, since the measurement is based on a handmade inductor, measurement results are affected by how an inductor is made. If many core samples are measured, repeatability can be a problem due to variation of coil winding.

The measured results in Figure 5 (VNA) have good agreement with characteristics presented Figure 8 (LCZ), in frequency range from 300 kHz to 1 MHz.

Technically, maximal operating temperature of ferrite material is its sintering temperature, i.e., the temperature at which the ferrite becomes reactive with the oxygen (usually in the around 900°C). We

can conclude from the above mentioned fact that ferrite materials could be the best choice for the devices that operate on high temperatures. However, some limitations should be taken into account, such as: Curie temperature, thermal shock and temperature variation of losses, permeability and magnetic flux saturation. The Curie temperature is typically between 140°C and 300°C for soft ferrites. Many ferrite features depend on temperature variation such as permeability. Because of that, additional permeability measurements were performed in the same frequency range, but at various temperatures. Figure 9 shows variation of real and imaginary parts of the permeability spectra with temperature (at 27°C, 50°C, 70°C, 100°C, and 120°C) for ESL 40012.

It was found that the real part of the permeability Re(μ) increases with rising temperature up to 70°C and after 100°C starts to decrease. Imaginary part of the permeability Im(μ) slightly increase at 50°C but after 70°C it start to decrease with increasing temperature.

5. DETERMINATION OF THE COMPLEX PERMEABILITY SPECTRA

Using the developed model, all dispersion parameters can be determined by numerical fitting to specified curves. For faster determination of dispersion parameters special software was developed.

Developed software tool offers the possibility of quick determination of dispersion parameters by comparing fitted permeability characteristic with measured permeability characteristic. Results of fitting, with developed software, are presented in Figure 10, where Re(μ)m

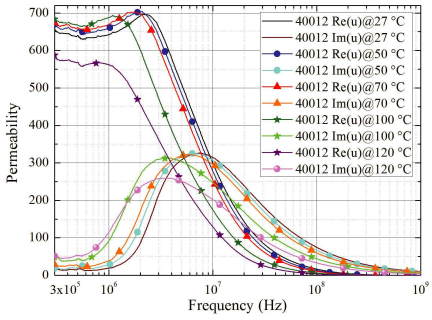

Figure 9. Complex permeability of LTCC sample measured at various temperatures.

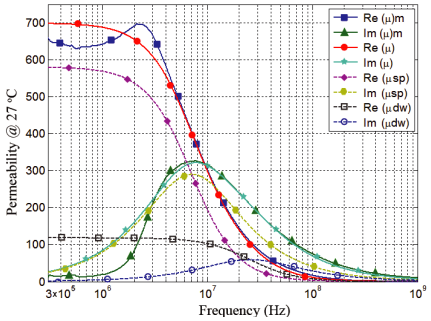

Figure 10. Comparison between measured and fitted permeability data for ESL 40012 at room temperature.

and Im(μ)m are measured real and imaginary parts of permeability; Re(μ) and Im(μ) are fitted real and imaginary parts of permeability; Re(μsp) and Im(μsp) are real and imaginary parts of spin permeability; Re(μdw) and Im(μdw) are real and imaginary parts of domain wall

Table 1. Dispersion parameters.

ESL 40012	K_{spin}	ω_{spin}^{res}	K_{dw}	ω_{dw}^{res}	β
@ 27°C	590	7 MHz	118	63,2 MHz	$155,7 \times 10^6$
@ 50°C	591	6,5 MHz	118	60 MHz	150×10^6
@ 70°C	590,5	5,8 MHz	118	58 MHz	$143,4 \times 10^6$
@ 100°C	580	3,9 MHz	115	38 MHz	$70,8 \times 10^6$
@ 120°C	490	3,6 MHz	88	35 MHz	70×10^6

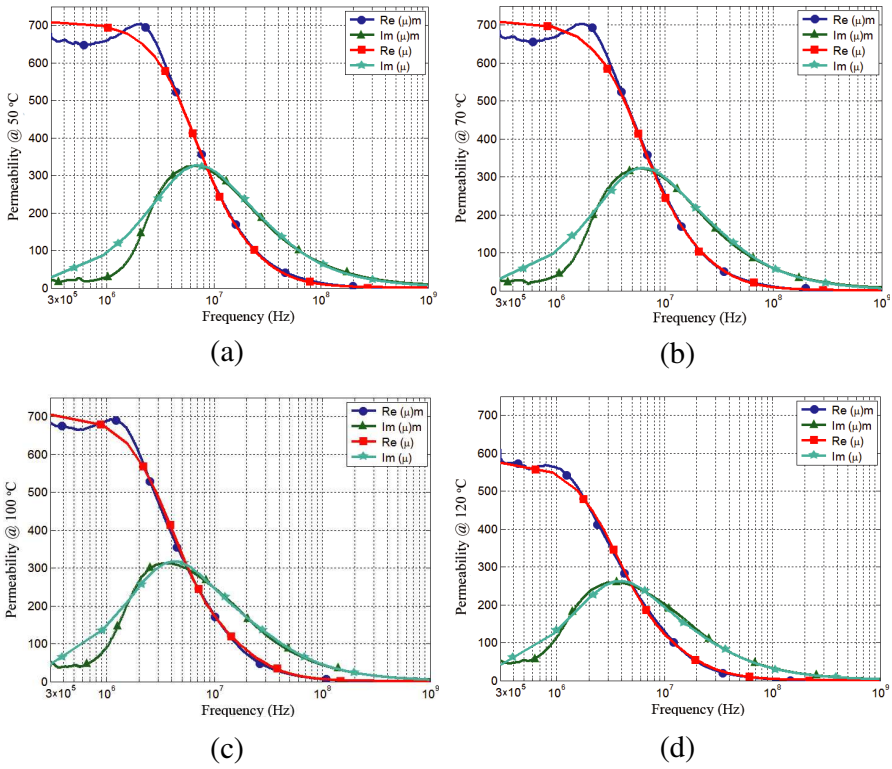

Figure 11. Comparison of measured and fitted characteristics at (a) 50 °C, (b) 70 °C, (c) 100 °C and (d) 120 °C.

permeability.

Measured results and fitted characteristics as can be seen have good match in the frequency range from 50 MHz to 1 GHz, implying accuracy of the presented model in this frequency range. The real and imaginary parts of measured and fitted characteristics intersect at the same frequency, 9,3 MHz.

For further analysis with the proposed model, the dispersion parameters are determined at various temperatures. Table 1 shows fitted values of dispersion parameters, which coincide the best with experimental curves given in Figure 9.

Temperature dependence of Re(μ) and Im(μ) with fitted charachteristic are presented in Figure 11. Fitted charachteristic have good match with measured charachteristic up to 120°C. At higher temperatures, fitted characteristic are possible to match with measured characteristic and determine dispersion parameters at frequency of interest.

6. COMPARISON OF LTCC AND CONVENTIONAL FERITE CORE

For further analysis, the LTCC ferrite toroid was compared with conventional ferrite core Neosid F19, [30]. This conventional, commercially available, ferite core was chosen for comparison with LTCC core because it is based on the same material, nickel-zinc ferrite.

As can be seen from presented graphs Figures 12 and 13, F19 core have greater value of permeability, but ESL 40012 can also be used at higher frequency and temperature.

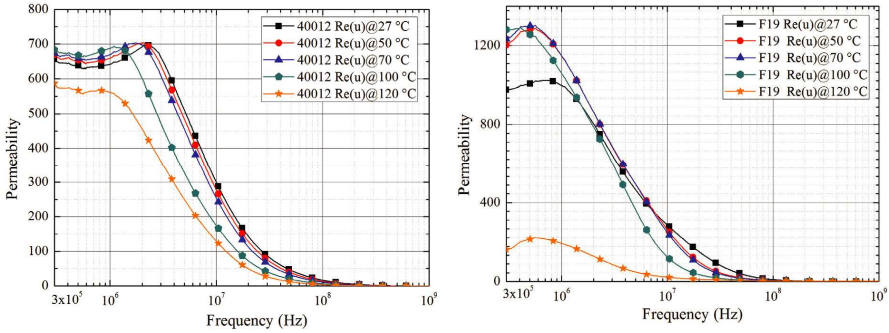

Figure 12. Temperature variation of Re(μ) for LTCC core (a) and conventional F19 core (b).

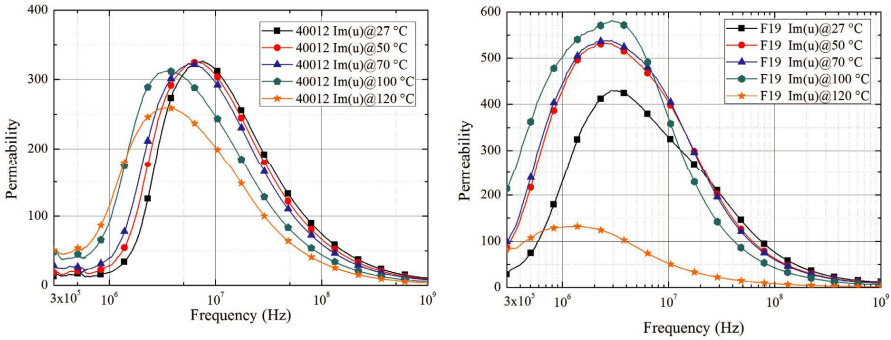

(a) (b)

Figure 13. Temperature variation of Im(μ) for LTCC core (a) and conventional F19 core (b).

7. CONCLUSION

This paper presents for the first time the characterization of a ferrite toroid sample of ESL 40012 LTCC ferrite tape, in the wide frequency range at various temperatures. A dispersion model for a better characterization of material was presented. The sample was fabricated with the conventional LTCC technology. The complex permeability of the toroidal sample was determined using a short circuit coaxial sample holder and vector network analyzer. Obtained measurement results show good agreement when they are compared with available catalog characteristics (permeability at 100 kHz is higher than 450). In addition, permeability was determined at various temperatures. Based on the dispersion model special software for determination of dispersion parameters was developed. Dispersion parameters are determined by numerical fitting of the obtained experimental results. Also, comparison with commercial available ferrite core was made. All results show good agreement with measured values.

ACKNOWLEDGMENT

This work is done within the scope of two projects EUREKA project, No. E!4570. and TR11023.

REFERENCES

1. Weir, W. B., "Automatic measurement of complex dielectric constant and permeability at microwave frequencies," *Proc. of the*

IEEE, Vol. 62, 1972.

2. Hewlett-Packard Product Note No. 8510-3.
3. Chukhov, V., "Methodic of magnetic permeability measurement," *14th International Crimean Conference on Microwave and Telecommunication Technology*, 680–681, CriMico, Sept. 2004.
4. Bussey, H. B., "Measurment of RF properties of materials a survey," *Proc. of The IEEE*, Vol.55, No. 6, 1046–1053, 1967.
5. Barry, W., "A broad-band, automated, stripline techniques for the simultaneous measurement of complex permittivity an permeability," *IEEE Trans. on MTT*, Vol. 34, No. 1, 80–84, 1986.
6. Jarvis, J. B., M. D. Janezic, B. F. Riddle, R. T. Johnk, R. Kabos, C. L. Holloway, R. G. Geyer, and C. A. Grosvenor, "Measuring the permittivity and permeability of lossy materials: Solids, liquids, metals, building materials, and negative-index materials," NIST Technical Note 1536, Boulder, CO, 2005.
7. Wu, Y. Q., Z. X. Tang, Y. H. Xu, and B. Zhang, "Measuring complex permeability of ferromagnetic thin films using microstrip transmission method," *Journal of Electromagnetic Waves and Applications*, Vol. 23, No. 10, 1303–1311, 2009.
8. Naishadham, K., "A rigorous experimental characterization of ferrite inductors for RF noise suppression," *1999 IEEE Radio and Wireless Conf., RAWCON 99*, 271–274, Denver, CO, Aug. 1999.
9. Yu, Q., T. W. Holmes, and K. Naishadham, "RF equivalent circuit modeling of ferrite-core inductors and characterization of core materials," *IEEE Trans. Electromagn. Compat.*, Vol. 44, No. 1, 258–262, Feb. 2002.
10. Foo, C. F. and D. M. Zhang, "A resonant method to construct core loss of magnetic materials using impedance analyzer," *PESC 98 Record 29th Ann. IEEE Power Electronics Specialists Conf.*, Vol. 2, 1997–2002, Fukuoka, Japan, May 1998.
11. Shenhui, J. and J. Quanxing, "An alternative method to determine the initial permeability of ferrite core using network analyzer," *IEEE Trans. on EMC*, Vol. 47, No. 3, 651–657, 2005.
12. Dosoudil, R., E. Ušak, and V. Olah, "Computer controlled system for complex permeability measurement in the frequency range of 5 Hz–1 GHz," *Journal of Electrical Engineering*, Vol. 57, No. 8/S, 105–109, 2006.
13. *Agilent 16454A Magnetic Material Test Fixture Operation and Service Manual*, 5th Edition, No. 16454-90020, Agilent Tech. Rep., Agilent Technologies, Inc., Palo Alto, CA, Jul. 2001.
14. Huang, R. and D. Zhang, "Application of mode matching method

to analysis of axisymmetric coaxial discontinuity structures used in permeability and/or permittivity measurement," *Progress In Electromagnetics Research*, Vol. 67, 205–230, 2007.

15. Huang, J., K. Wu, P. Morin, and C. Akgel, "Characterization of highly dispersive materials using composite coaxial cells: Electromagnetic analysis and wideband measurement," *IEEE Trans. on MMT*, Vol. 44, No. 5, 770–777, 1996.
16. Zhang, D. M. and C. F. Foo, "Theoretical analysis of the electrical and magnetic field distribution in a toroidal core with circular cross section," *IEEE Trans. on Mag.*, Part 2, Vol. 33, No. 3, 1924–1931, 1999.
17. Hacivelioglu, F. and A. Büyükaksoy, "Wiener-hopf analysis of finite-length impedance loading in the outer conductor of a coaxial waveguide," *Progress In Electromagnetics Research B*, Vol. 5, 241–251, 2008.
18. Jiang, H. and R.-M. Xu, "9.5 GHz 16λg delay line using multilayer LTCC," *Progress In Electromagnetics Research Letters*, Vol. 6, 175–182, 2009.
19. Lee, Y. C., "CPW-to-stripline vertical via transitions for 60 GHz LTCC SoP applications," *Progress In Electromagnetics Research Letters*, Vol. 2, 37–44, 2008.
20. Lee, Y. C. and T. W. Kim, "A low-loss patch LTCC bpf for 60 GHz system-on-package (SoP) applications," *Progress In Electromagnetics Research Letters*, Vol. 12, 183–189, 2009.
21. Gu, J., Y. Fan, and Y. Zhang, "A X-band 3-D SICC filter with low-loss and narrow band using LTCC technology," *Journal of Electromagnetic Waves and Applications*, Vol. 23, No. 8–9, 1093–1100, 2009.
22. Matters-Kammerer, M., et al., "Material propoerties and RF applications of high k and ferrite LTCC ceramics," *Microelectronics and Reliability*, 134–143, Jan. 2006.
23. Slama, G., "Low-temperature sintering of Ni-Zn-Cu ferrite and its permeability spectra," *Power Electronics and RF Applications*, 30–34, Jan. 2003.
24. Wahlers, R. L., C. Y. D. Huang, M. R. Heinz, A. H. Feingold, J. Bielawski, and G. Slama, "Low profile LTCC transformers," available at www.electroscience.com/publications/IMAPS2002-(1).pdf.
25. ESL ElectroScience, http://www.electroscience.com.
26. Schlomann, E., "Microwave behavior of partially magnetized ferrites," *J. Appl. Phys.*, Vol. 41, No. 1, 204–214, 1970.

27. Tsutaoka, T., M. Ueshima, and T. Tokunaga, "Frequency dispersion and temperature variation of complex permeability of Ni-Zn ferrite composite materials," *J. Appl. Phys.*, Vol. 78, No. 6, 3983–3991, 1995.
28. Tsutaoka, T., "Frequency dispersion of complex permeability in Mn-Zn and Ni-Zn spinel ferrites and their composite materials," Vol. 93, No. 5, 2789–2796, Mar. 2003.
29. Radonić, V., N. Blaž, and L. Živanov, "Measurement of complex permeability using short coaxial line reflection method," *Acta Physica Polonica*, Vol. 117, No. 4, 820–824, 2010.
30. MMG-Neosid, http://www.mmgca.com.